

Neutron stars and quark phases in the Nambu–Jona-Lasinio model

Klaus Schertler* and Stefan Leupold

Institut für Theoretische Physik, Universität Giessen, D-35392 Giessen, Germany

Jürgen Schaffner-Bielich

RIKEN BNL Research Center, Brookhaven National Laboratory, Upton, New York 11973-5000

(Received 14 January 1999; published 30 June 1999)

We study the possible existence of deconfined quark matter in the interior of neutron stars using the Nambu–Jona-Lasinio model to describe the quark phase. We find that typical neutron stars with masses around 1.4 solar masses do not possess any deconfined quark matter in their center. This can be traced back to the property of the NJL model which suggests a large constituent strange quark mass over a wide range of densities. [S0556-2813(99)01008-0]

PACS number(s): 26.60.+c, 12.39.-x, 12.38.Mh

I. INTRODUCTION

At large temperatures or large densities hadronic matter is expected to undergo two phase transitions: one which deconfines quarks (and gluons) and one which restores chiral symmetry. Up to now it is an unsettled issue whether these two phase transitions are distinct or coincide. Moreover, it is even unclear whether there are real phase transitions or only rapid crossover transitions. Such transitions have received much attention in heavy ion physics as well as in the context of neutron stars which provide a unique environment to study cold matter at supernuclear densities [1,2]. Even though a deconfinement phase transition seems intuitively evident at large enough densities, from a theoretical point of view a confirmation of the existence of a deconfined quark phase in neutron stars is so far limited by the uncertainties in modeling QCD at large densities. All the more it is important to study and compare different available models to shed some light on similarities and differences with respect to the behavior of matter at large densities as well as on the corresponding predictions of neutron star properties like, e.g., its mass and radius. In the future such experience may prove to be useful if either an improved understanding of matter under extreme conditions provides a more exclusive selection between the various models or new experimental results on neutron star properties are available to set more stringent constraints.

Usually the quark matter phase is modeled in the context of the MIT bag model [2–4] as a Fermi gas of u , d , and s quarks. In this model the phenomenological bag constant B_{MIT} is introduced to mimic QCD interactions to a certain degree. The investigation of such a phase was furthermore stimulated by the idea that a quark matter phase composed of almost an equal amount of the three lightest quark flavors could be the ground state of nuclear matter [2,4–7]. Indeed, for a wide range of model parameters such as the bag constant, bag models predict that the quark matter phase is absolutely stable, i.e., its energy per baryon at zero pressure is lower than the one of ^{56}Fe . If this is true, this has important

consequences in physics and astrophysics [7] leading, e.g., to the possibility of so called “strange stars” [2,7] which are neutron stars purely consisting of quark matter in weak equilibrium with electrons. Of course, to check the model dependence of such findings it is important to perform the corresponding calculations also in models different from the MIT bag model. In a recent work by Buballa and Oertel [8] the equation of state (EOS) of quark matter was investigated in the framework of the Nambu–Jona-Lasinio (NJL) model with three quark flavors. Applying this model it was found that strange quark matter is not absolutely stable. This would rule out the existence of strange stars. On the other hand, the possibility of quark phases in the interior of neutron stars is in principle not excluded by this result—even though this possibility gets energetically less likely. Only a detailed phase transition calculation can answer the question which effect the findings in [8] have on the existence of quark phases inside neutron stars. This is what we are aiming at in the present work.

In principle, for the description of a neutron star which consists of a quark phase in its center and a surrounding hadronic phase (and, as we shall discuss below, a mixed phase in between) we need models for both phases. The most favorite case would be to have one model which can reliably describe both phases. So far, there are no such models. Therefore, we will use various versions of the relativistic mean field model to parametrize the hadronic phase. For the quark phase we follow Buballa and Oertel [8] in using the three-flavor version of the NJL model. The NJL model has proved to be very successful in the description of the spontaneous breakdown of chiral symmetry exhibited by the true (nonperturbative) QCD vacuum. It explains very well the spectrum of the low lying mesons which is intimately connected with chiral symmetry as well as many other low energy phenomena of strong interaction [9–11]. At high enough temperature and/or density the NJL model predicts a transition to a state where chiral symmetry becomes restored. Despite that promising features which at first sight might suggest the NJL model as a good candidate for modeling both the low and high density region of a neutron star this model has one important shortcoming, namely it does not confine quarks. At low densities, however, the bulk proper-

*Electronic address: klaus.schertler@theo.physik.uni-giessen.de

ties of strongly interacting matter are significantly influenced by the fact that quarks are confined there. Therefore, we cannot expect that the NJL model gives reliable results for the EOS at low densities. Thus we will use the relativistic mean field model to describe the confined phase. At higher densities, however, the quarks are expected to be deconfined. There we expect the NJL model to be applicable since the lack of confinement inherent to this model is irrelevant in that regime. The interesting feature of the NJL model is that it reflects the chiral symmetry of QCD. Clearly, it would be preferable to have a Lagrangian for the hadronic phase which also respects chiral symmetry like, e.g., the one constructed in [12] for the two-flavor case and the SU(3) generalizations [13,14]. Such Lagrangians, however, are more complicated to deal with. First applications to neutron star matter seem to indicate that the modifications are rather small as compared to the relativistic mean field models used here [15]. For simplicity, we therefore will restrict our considerations to the much simpler extensions of the Walecka model which include hyperonic degrees of freedom (relativistic mean field models).

The paper is organized as follows: In Sec. II we discuss how the EOS for the hadronic phase of a neutron star is calculated within several variants of relativistic mean field models. We keep brief here since such models are frequently used and well documented in the literature (cf., e.g., [2]). In Sec. III we apply the NJL model to the description of the possible quark phase of the neutron star. Here we present much more details as compared to Sec. II since to the best of our knowledge it is the first time that the NJL model is applied to the description of the quark phase in a neutron star. Section IV is devoted to the construction of the phase transition and to the application of the complete EOS to the internal structure of the neutron star. Finally we summarize and discuss our results in Sec. V.

II. HADRONIC MATTER

Neutron stars cover a wide range of densities. From the surface of the star which is composed of iron with a density of $\epsilon \approx 8 \text{ g/cm}^3$ the density can increase up to several times normal nuclear matter density ($\epsilon_0 = 140 \text{ MeV/fm}^3 \approx 2.5 \times 10^{14} \text{ g/cm}^3$) in the center of the star. Since there is no single theory that covers this huge density range, we are forced to use different models to meet the requirements of the various degrees of freedom opened up at different densities. For subnuclear densities we apply the Baym-Pethick-Sutherland EOS [16]. The degrees of freedom in this EOS are nuclei, electrons and neutrons. The background of neutrons appears above neutron drip density ($\epsilon_{\text{drip}} \approx 4 \times 10^{11} \text{ g/cm}^3$) when the most weakly bound neutrons start to drip out of the nuclei which themselves get more and more neutron rich with increasing density. For a detailed discussion of the Baym-Pethick-Sutherland EOS see also [1]. We also refer to [17] where a relativistic mean field model is extended to also describe this low density range.

At densities of about normal nuclear density ϵ_0 the nuclei begin to dissolve and merge together and nucleons become

TABLE I. Nuclear matter properties of the hadronic EOS's. The saturation density and the binding energy is denoted by ρ_0 and B/A , the incompressibility by K , the effective mass by m_N^*/m_n , and the symmetry energy by a_{sym} . The particle compositions are shown at the bottom of the table.

Hadronic EOS	TM1	TM2	GL85	GPS
Reference	[20]	[20]	[20]	[21]
ρ_0 [fm^{-3}]	0.145	0.132	0.145	0.150
B/A [MeV]	-16.3	-16.2	-15.95	-16.0
K [MeV]	281	344	285	300
m_N^*/m_n	0.634	0.571	0.770	0.830
a_{sym} [MeV]	36.9	35.8	36.8	32.5
Composition	a	a	a	b
(a) $n, p, e^-, \mu^-, \Lambda, \Sigma^-, \Sigma^0, \Sigma^+, \Xi^-, \Xi^0$				
(b) $n, p, e^-, \mu^-, \Lambda, \Sigma^-$				

the relevant degrees of freedom in this phase. We want to describe this phase in the framework of the relativistic mean field (RMF) model which is widely used for the description of dense nuclear matter [18–20]. For an introduction to the RMF model see, e.g., [2]. We use three EOS's calculated by Schaffner and Mishustin in the extended RMF model [20] (denoted as TM1, TM2, GL85) and one by Ghosh, Phatak, and Sahu [21]. For the latter one we use GPS as an abbreviation. These models include hyperonic degrees of freedom which typically appear at $\epsilon \approx 2-3\epsilon_0$. Table I shows the nuclear matter properties and the particle composition of the four EOS's. The RMF EOS's are matched to the Baym-Pethick-Sutherland EOS at densities of $\epsilon \approx 10^{14} \text{ g/cm}^3 \approx \epsilon_0$. Even if the relevant degrees of freedom are specified (in the RMF case basically nucleons and hyperons) the high density range of the EOS is still not well understood. The use of different hadronic models should reflect this uncertainty to some degree. In the following we denote the phase described by the Baym-Pethick-Sutherland EOS and by the RMF model as the *hadronic phase* (HP) of the neutron star.

III. QUARK PHASE

To describe the deconfined *quark phase* (QP) we use the Nambu–Jona-Lasinio (NJL) model [22] with three flavors [23] in Hartree (mean field) approximation (for reviews on the NJL model cf. [9–11]). The Lagrangian is given by (cf. [8,23])

$$\mathcal{L} = \bar{q}(i\partial - \hat{m})q + G \sum_{k=0}^8 [(\bar{q}\lambda_k q)^2 + (\bar{q}i\gamma_5\lambda_k q)^2] - K[\det_f(\bar{q}(1 + \gamma_5)q) + \det_f(\bar{q}(1 - \gamma_5)q)], \quad (1)$$

where q denotes a quark field with three flavors, u , d , and s , and three colors. $\hat{m} = \text{diag}(m_u, m_d, m_s)$ is a 3×3 matrix in flavor space. For simplicity we use the isospin symmetric case, $m_u = m_d \equiv m_q$. The λ_k matrices act in flavor space. For $k=1, \dots, 8$ they are the generators of $SU(3)_f$ while λ_0 is proportional to the unit matrix in flavor space (see [10] for

details). The four-point interaction term $\sim G$ is symmetric in $SU_V(3) \times SU_A(3) \times U_V(1) \times U_A(1)$. In contrast, the determinant term $\sim K$ which for the case of three flavors generates a six-point interaction breaks the $U_A(1)$ symmetry. If the mass terms are neglected the overall symmetry of the Lagrangian therefore is $SU_V(3) \times SU_A(3) \times U_V(1)$. In vacuum this symmetry is spontaneously broken down to $SU_V(3) \times U_V(1)$ which implies the strict conservation of baryon and flavor number. The full chiral symmetry—which implies in addition the conservation of the axial flavor current—becomes restored at sufficiently high temperatures and/or densities. The finite mass terms introduce an additional explicit breaking of the chiral symmetry. On account of the chiral symmetry breaking mechanism the quarks get constituent quark masses which in vacuum are considerably larger than their current quark mass values. In media with very high quark densities constituent and current quark masses become approximately the same (concerning the strange quarks this density regime lies far beyond the point where chiral symmetry is restored).

The coupling constants G and K appearing in Eq. (1) have dimension energy $^{-2}$ and energy $^{-5}$, respectively. To regularize divergent loop integrals we use for simplicity a sharp cutoff Λ in 3-momentum space. Thus we have at all five parameters, namely the current quark masses m_q and m_s , the coupling constants G and K , and the cutoff Λ . Following [23] we use $\Lambda = 602.3$ MeV, $G\Lambda^2 = 1.835$, $K\Lambda^5 = 12.36$, $m_q = 5.5$ MeV, and $m_s = 140.7$ MeV. These parameters are chosen such that the empirical values for the pion decay constant and the meson masses of pion, kaon and η' can be reproduced. The mass of the η meson is underestimated by about 6%.

We treat the three-flavor NJL model in the Hartree approximation which amounts to solve in a self-consistent way the following gap equations for the dynamically generated constituent (effective) quark masses:

$$m_i^* = m_i - 4G\langle\bar{q}_i q_i\rangle + 2K\langle\bar{q}_j q_j\rangle\langle\bar{q}_k q_k\rangle, \quad (2)$$

with (i, j, k) being any permutation of (u, d, s) . At zero temperature but finite quark chemical potentials the quark condensates are given by

$$\begin{aligned} \langle\bar{q}_i q_i\rangle &= -2N_c \int_{p_F^i < |\vec{p}| < \Lambda} \frac{d^3 p}{(2\pi)^3} \frac{m_i^*}{\sqrt{(m_i^*)^2 + p^2}} \\ &= -\frac{3}{\pi^2} \int_{p_F^i}^{\Lambda} dp p^2 \frac{m_i^*}{\sqrt{(m_i^*)^2 + p^2}}, \end{aligned} \quad (3)$$

where we have taken the number of colors to be $N_c = 3$. p_F^i denotes the Fermi momentum of the respective quark flavor i . It is connected with the respective quark chemical potential μ_i via

$$p_F^i = \sqrt{\mu_i^2 - (m_i^*)^2} \Theta(\mu_i - m_i^*). \quad (4)$$

The corresponding quark particle number density is given by and

$$\rho_i = 2N_c \int_{|\vec{p}| < p_F^i} \frac{d^3 p}{(2\pi)^3} = \frac{(p_F^i)^3}{\pi^2}. \quad (5)$$

For later use we also introduce the baryon particle number density

$$\rho \equiv \frac{1}{3}(\rho_u + \rho_d + \rho_s). \quad (6)$$

Equations (2) and (3) serve to generate constituent quark masses which decrease with increasing densities from their vacuum values of $m_{q,\text{vac}}^* = 367.7$ MeV and $m_{s,\text{vac}}^* = 549.5$ MeV, respectively.

Before calculating the EOS we would like to comment briefly on the Hartree approximation to the NJL model which we use throughout this work. This treatment is identical to a leading order calculation in the inverse number of colors $1/N_c$ [10]. In principle, one can go beyond this approximation by taking into account $1/N_c$ corrections in a systematic way. This amounts in the inclusion of quark-antiquark states (mesons) as RPA modes in the thermodynamical calculations [24,25]. Several things then change: First of all, these mesons might contribute to the EOS. We are not aware of a thorough discussion of such an EOS for three flavors with finite current quark masses. The two-flavor case is discussed in [25]. Qualitatively the masses of the meson states rise above the chiral transition point. Therefore, they should become energetically disfavored and thus less important. An additional technical complication arises due to the fact that the relation between the Fermi energy and the chemical potential becomes nontrivial. Instead of Eq. (4) one has to solve an additional gap equation for each flavor species. These gap equations are coupled to the gap equations for the constituent quark masses given in Eq. (2). We refer to [10] for details. For simplicity we will restrict ourselves in the following to the Hartree approximation and comment on the possible limitations of that approach in the last section.

Coming back to the EOS we also need the energy density and the pressure of the quark system. In the Hartree approximation the energy density turns out to be [8]

$$\epsilon_{\text{NJL}} = \sum_{i=u,d,s} \frac{3}{\pi^2} \int_0^{p_F^i} dp p^2 \sqrt{(m_i^*)^2 + p^2} + B_{\text{eff}}, \quad (7)$$

while pressure and energy density are related via

$$p_{\text{NJL}} + \epsilon_{\text{NJL}} = \sum_{i=u,d,s} \rho_i \mu_i, \quad (8)$$

where the effective bag pressure B_{eff} is given by

$$B_{\text{eff}} = B_0 - B, \quad (9)$$

with

$$\begin{aligned} B &= \sum_{i=u,d,s} \left[\frac{3}{\pi^2} \int_0^{\Lambda} dp p^2 (\sqrt{(m_i^*)^2 + p^2} - \sqrt{(m_i)^2 + p^2}) \right. \\ &\quad \left. - 2G\langle\bar{q}_i q_i\rangle^2 \right] + 4K\langle\bar{u}u\rangle\langle\bar{d}d\rangle\langle\bar{s}s\rangle \end{aligned} \quad (10)$$

$$B_0 = B|_{\rho_u = \rho_d = \rho_s = 0} = (217.6 \text{ MeV})^4. \quad (11)$$

Note that B depends implicitly on the quark densities via the (density dependent) constituent quark masses. The appearance of the density independent constant B_0 ensures that energy density and pressure vanish in vacuum. We note here that this requirement fixes the density independent part of B_{eff} which influences the EOS via Eqs. (7) and (8) and therefore the possible phase transition to quark matter. We will come back to this point in the last section. In what follows we shall frequently compare the results of the three-flavor NJL model with the simpler MIT bag model [3,4]. For that purpose it is important to realize that the NJL model predicts a (density dependent) bag pressure B_{eff} while in the MIT bag model the bag constant B_{MIT} is a density independent free parameter. There usually also the quark masses m_i^{MIT} are treated as density independent quantities. (An exception is the model discussed in [26,27] which uses density dependent effective quark masses caused by quark interactions in the high density regime.) In the bag model energy density and pressure of the quark system are given by

$$\epsilon_{\text{MIT}} = \sum_{i=u,d,s} \frac{3}{\pi^2} \int_0^{p_F^i} dp p^2 \sqrt{(m_i^{\text{MIT}})^2 + p^2} + B_{\text{MIT}} \quad (12)$$

and

$$p_{\text{MIT}} + \epsilon_{\text{MIT}} = \sum_{i=u,d,s} \rho_i \mu_i. \quad (13)$$

Suppose now that the densities are so high that in the three-flavor NJL model the effective quark masses have dropped down to the current quark masses. In this case, energy density and pressure take the form of the respective expressions in the MIT bag model with $m_i^{\text{MIT}} = m_i$ and $B_{\text{MIT}} = B_0$. However, a word of caution is in order here. For *very high* quark particle number densities the corresponding Fermi momenta become larger than the momentum cut-off Λ introduced to regularize the NJL model. In this case the results of the NJL model become unreliable. For example, the upper limit of the momentum integration in Eq. (5) would be no longer given by the Fermi momentum but by the cutoff Λ which would be clearly an unphysical behavior of the model. Thus for all practical purposes one should always ensure that in the region of interest the Fermi momenta are smaller than the momentum cutoff Λ . Figure 1 shows the Fermi momenta of the quarks as a function of the baryon particle number density (for a charge neutral system of quarks and electrons in weak equilibrium; cf. next paragraph for details). Obviously all Fermi momenta stay below the cutoff Λ for the shown region. We will come back to that point at the end of this section. As we shall see below concerning the properties of typical neutron stars we only need the QP EOS up to densities of about $3\rho_0$ where according to Fig. 1 the Fermi momenta stay well below the cutoff Λ .

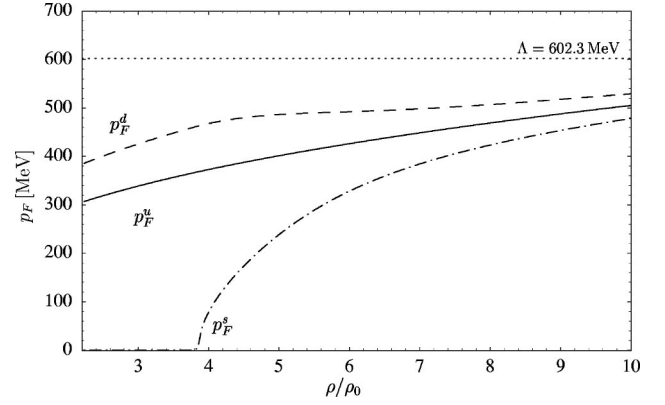
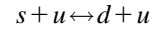
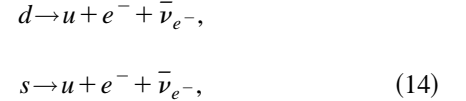


FIG. 1. Fermi momenta of the quarks as a function of baryon particle number density for a charge neutral system of quarks and electrons in weak equilibrium. Λ denotes the cutoff introduced to regularize the NJL model. $\rho_0 = 0.17 \text{ fm}^{-3}$ denotes nuclear saturation density.

The QP which might be found in the center of a neutron star consists of u , d , and s quarks and electrons in weak equilibrium, i.e., the weak reactions



imply relations between the four chemical potentials $\mu_u, \mu_d, \mu_s, \mu_e$ which read

$$\mu_s = \mu_d = \mu_u + \mu_e. \quad (15)$$

Since the neutrinos can diffuse out of the star their chemical potentials are taken to be zero. The number of chemical potentials necessary for the description of the QP in weak equilibrium is therefore reduced to *two* independent ones. For convenience we choose the pair (μ_n, μ_e) with the neutron chemical potential

$$\mu_n \equiv \mu_u + 2\mu_d. \quad (16)$$

In a pure QP (in contrast to quark matter in a mixed phase which we will discuss later) we can require the QP to be charge neutral. This gives us an additional constraint on the chemical potentials via the following relation for the particle number densities:

$$\frac{2}{3}\rho_u - \frac{1}{3}\rho_d - \frac{1}{3}\rho_s - \rho_e = 0, \quad (17)$$

where ρ_e denotes the electron particle number density. Neglecting the electron mass it is given by

$$\rho_e = \frac{\mu_e^3}{3\pi^2}. \quad (18)$$

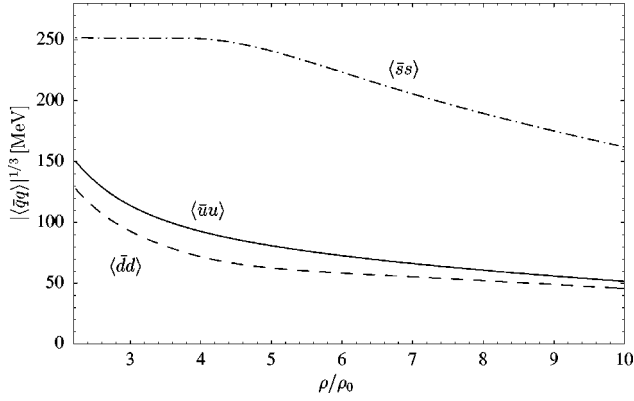


FIG. 2. Quark condensates as a function of baryon particle number density for a charge neutral system of quarks and electrons in weak equilibrium. Note that all condensates have negative values [cf. Eq. (3)].

Utilizing the relations (15) and (17) the EOS can now be parametrized by only *one* chemical potential, say μ_n . At this point it should be noted that the arguments given here for the QP also holds for the HP. There one also ends up with *two* independent chemical potentials (e.g., μ_n and μ_e) if one only requires weak equilibrium between the constituents of the HP and with *one* chemical potential (e.g., μ_n) if one additionally requires charge neutrality. As we will discuss later, the number of independent chemical potentials plays a crucial role in the formulation of the Gibbs condition for chemical and mechanical equilibrium between the HP and the QP.

In the pure QP total energy density and pressure are given by the respective sums for the quark and the electron system, i.e.,

$$\epsilon = \epsilon_{\text{NJL}} + \frac{\mu_e^4}{4\pi^2} \quad (19)$$

and

$$p = p_{\text{NJL}} + \frac{\mu_e^4}{12\pi^2}, \quad (20)$$

where the system of electrons is treated as a massless ideal gas. One obtains the analogous expressions for the MIT bag model if ϵ_{NJL} and p_{NJL} are replaced by the respective MIT expressions (12) and (13).

Demanding weak chemical equilibrium (15) and charge neutrality (17) as discussed above all thermodynamic quantities as well as quark condensates, effective quark masses etc. can be calculated as a function of one chemical potential μ_n . The curves in Fig. 1 as well as in Figs. 2–7 which we shall discuss in the following are obtained by varying μ_n while obeying simultaneously the constraints (15) and (17).

Figures 2 and 3 show the quark condensates and the effective quark masses, respectively, as a function of the baryon particle number density. Note that we start already at a density as high as two times nuclear saturation density $\rho_0 = 0.17 \text{ fm}^{-3}$ since we want to describe only the high density

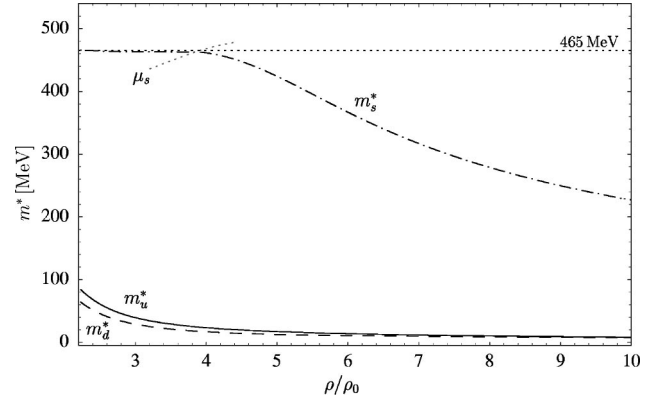


FIG. 3. Effective quark masses as a function of baryon particle number density for a charge neutral system of quarks and electrons in weak equilibrium. In addition the strange quark chemical potential μ_s is plotted in the region where it meets the constituent strange quark mass. This marks the point where strange quarks appear in the system (see also Fig. 1).

regime of the neutron star with quark degrees of freedom while for low densities we use the hadronic EOS described in the previous section. Concerning the low density regime of the three-flavor NJL model we refer to [8] for details. There it was shown that the energy per baryon of a charge neutral system of quarks and electrons in weak equilibrium (described by the NJL model and a free electron gas) shows a minimum somewhat above two times ρ_0 . This implies that in the density region below this minimum the pressure is negative. We are not interested in the (low density) part of the EOS with negative pressure since it cannot be realized in a neutron star. In the region of interest Figs. 2 and 3 show that the strange quark condensate and the effective strange quark mass stay constant until the strange chemical potential μ_s overwhelms the strange quark mass. Only then according to Eq. (4) the strange quark particle number density ρ_s and the corresponding Fermi momentum p_F^s (cf. Fig. 1) become different from zero causing a decrease of $|\langle \bar{s}s \rangle|$ and m_s^* . Note that all condensates have negative values [cf. Eq. (3)]. One might wonder why the dropping of the condensates of

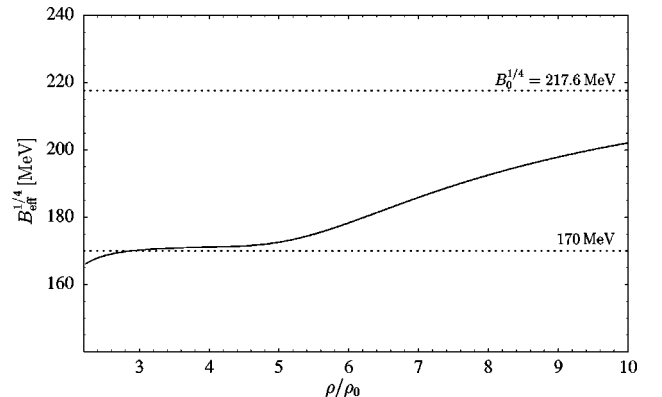


FIG. 4. The bag pressure (to the power of 1/4) as function of the baryon particle number density for the same conditions as described in Figs. 2 and 3.

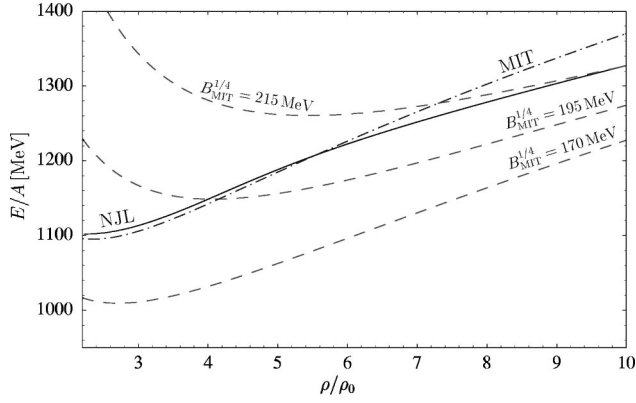


FIG. 5. Energy per baryon versus baryon particle number density for the NJL model and the MIT bag model for various values of the bag pressure and the strange quark mass. The curve labeled with “MIT” uses a bag pressure of $B_{\text{MIT}}^{1/4} = 170$ MeV and a strange quark mass of $m_s^{\text{MIT}} = 465$ MeV. All other bag model curves use the current strange quark mass of 140.7 MeV. See main text for details.

the light up and down quarks does not decrease the strange quark mass (and condensate) due to the last coupling term in Eq. (2). Indeed, strange quark mass and condensate have dropped in the low density region (not shown here) from their vacuum values down to the plateaus shown in Figs. 2 and 3 due to their coupling to the up and down quark condensates. In the plateau region, however, these condensates have already decreased so much that their influence on the strange quark mass is diminished. We refer to [8] for details. As we shall see below, the large plateau value of the strange quark mass will have considerable influence on the phase structure in the interior of neutron stars.

Figure 4 shows the bag pressure B_{eff} as a function of the baryon particle number density. After staying more or less constant up to roughly 5 times nuclear saturation density it starts to increase towards B_0 which, however, it will reach only very slowly. Again the rising of B_{eff} can be traced back to the strange quarks which come into play at high densities.

Thermodynamic quantities are shown in Figs. 5–7. For comparison various curves calculated within the MIT bag

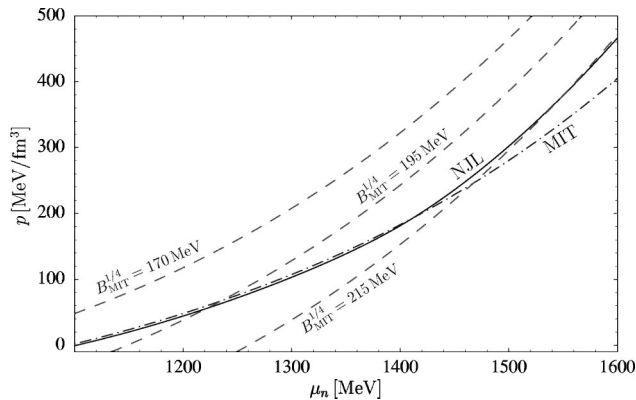


FIG. 6. Pressure versus neutron chemical potential for the NJL model and the MIT bag model for various values of the bag pressure and the strange quark mass. See Fig. 5 and main text for details.

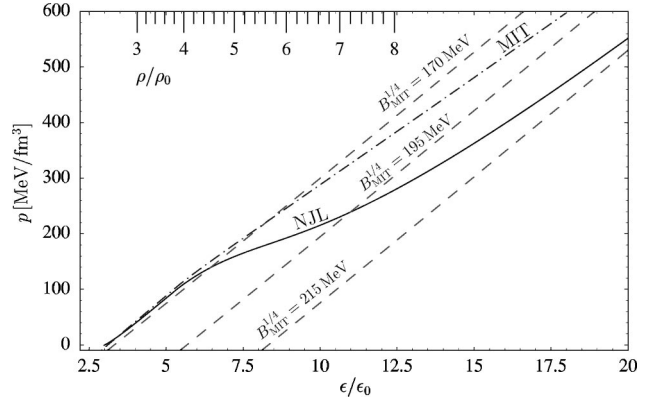


FIG. 7. Pressure versus energy density for the NJL model and the MIT bag model for various values of the bag pressure and the strange quark mass. The upper scale shows the corresponding particle number densities. $\epsilon_0 = 140$ MeV/fm³. See Fig. 5 and main text for details.

model are added. The curves labeled with a specific value of the bag pressure are obtained from Eqs. (12) and (13) in weak equilibrium where the respective value of B_{MIT} and the current quark masses $m_q = 5.5$ MeV and $m_s = 140.7$ MeV are used. In contrast to that for the curve labeled with “MIT” we have used the plateau values of the bag pressure $B_{\text{MIT}}^{1/4} = 170$ MeV (cf. Fig. 4) and of the strange quark mass $m_s^{\text{MIT}} = 465$ MeV (cf. Fig. 3). For up and down quarks we have used the current quark mass values also here. Figure 5 shows the energy per baryon as a function of the baryon particle number density. We find that the results of the NJL model calculation cannot be reproduced by a bag model using the current strange quark mass—no matter which bag pressure is chosen. As already discussed above, the reason simply is that in the NJL model up to four times ρ_0 there are no strange quarks in a system which is in weak equilibrium (cf. Fig. 1). On the other hand, in bag models using the much lower current strange quark mass one finds a reasonable amount of strange quarks already at vanishing pressure which typically corresponds to 2–3 times ρ_0 [26]. In contrast to that, a bag model with the plateau values for bag pressure and strange quark mass (denoted as “MIT” in the figures) yields a very good approximation to the NJL result for the energy per baryon up to 6–7 times ρ_0 . For higher particle number densities the NJL result bends over and can be better described by bag models using the current strange quark mass and higher bag pressures (roughly B_0). All these findings also apply to the interpretation of Fig. 6 which shows the total pressure of the system versus the baryon chemical potential. Comparing the two curves with the same bag constant labeled with “ $B_{\text{MIT}}^{1/4} = 170$ MeV” and with “MIT,” respectively, one observes that the latter one has a significantly lower pressure. This is due to the use of the much larger effective strange quark mass of $m_s^{\text{MIT}} = 465$ MeV in the latter case as compared to the current strange quark mass of 140.7 MeV used in the former. The p versus μ_n relation is an important ingredient for the construction of the phase transition from hadronic to quark matter inside a neutron star. We

note already here, however, that we need in addition the thermodynamical relations also for a quark-electron system away from the charge neutral configuration to describe correctly the phase transition (see below).

The outlined picture concerning the comparison of NJL and bag models is somewhat modified when looking at Fig. 7 which shows the total pressure as a function of the energy density. EOS's in the form $p(\epsilon)$ enter the Tolman-Oppenheimer-Volkoff [28] equation which in turn determines the mass-radius relation of neutron stars. We see that in the lower part of the plotted energy density range the EOS in Fig. 7 is reasonably well described by MIT bag models with the plateau value $B_{\text{MIT}}^{1/4} = 170$ MeV no matter which quark masses are chosen (current or effective quark masses). The reason is that the $p(\epsilon)$ relation is not very sensitive to the quark masses. This has already been observed in a somewhat different context in [26]. Going to higher densities the strange quarks enter the game and the EOS in Fig. 7 obtained from the NJL model starts to deviate from the EOS of the MIT bag models with the plateau value $B_{\text{MIT}}^{1/4} = 170$ MeV. For very high densities the pressure determined from the NJL model becomes comparable to the one calculated in the bag model with a high bag constant (roughly B_0). It is interesting to note that the deviation between the NJL curve and the "MIT" curve starts to increase in Fig. 7 much earlier than in Figs. 5 and 6. This shows that the pressure versus energy density relation is much more sensitive to the detailed modeling than the relations shown in Figs. 5 and 6.

Before constructing the phase transition inside the neutron star let us briefly discuss the limitations of the NJL model in the form as we have treated it here. As a typical low energy theory the NJL model is not renormalizable. This is not an obstacle since such theories by construction should be only applied to low energy problems. In practice the results depend on the chosen cutoff or, to turn the argument around, the NJL model is only properly defined once a cutoff has been chosen. This cutoff serves as a limit for the range of applicability of the model. Here we have used one cutoff Λ for the three-momenta of all quark species. Concerning the discussion of other cutoff schemes and their interrelations we refer to [10,11]. When the density in the quark phase gets higher the Fermi momenta of the quarks rise due to the Pauli principle. Eventually they might overwhelm the cutoff of the NJL model. At least beyond that point the model is no longer applicable. We have made sure in our calculations that this point is never reached (cf. Fig. 1). Nevertheless, by inspection of Fig. 1 one finds that the cutoff and the Fermi momenta have the same order of magnitude. Thus, the cutoff is comparatively small, i.e., it is not much larger than the typical momenta under consideration. Owing to the smallness of the cutoff the obtained results should be interpreted with care. Consequently we will check in Sec. V the sensitivity of our results to an artificial increase of the cutoff.

In addition, at very high densities one presumably enters a regime which might be better described by (resummed) perturbation theory. While the nonperturbative features of the NJL model vanish with rising density, medium effects as mediated, e.g., by one-gluon exchange grow with the density [26,27]. To summarize, concerning the calculation of the

EOS it turns out that the NJL model should neither be used at low densities where confinement properties are important nor at very high densities where the NJL model as a low energy theory leaves its range of applicability. However, the NJL model might yield reasonable results in a window of the density range where confinement is no longer crucial but chiral symmetry as a symmetry of full QCD remains to be important.

IV. PHASE TRANSITION AND NEUTRON STARS

In the previous sections we have discussed the underlying EOS's thought to reflect the properties of confined hadronic matter (HP) and deconfined quark matter (QP) in its particular regime of applicability. Applying these EOS's we want to calculate in this section the phase transition from the HP to the QP to see which phase is the favored one at which densities. (The existence of a QP inside the neutron star of course requires the phase transition density to be smaller than the central density of the star.)

It is worth to point out which phase structure is in principle possible if a hadronic model and the NJL model are connected at a certain density value ρ_{deconf} (which is dynamically determined in the present work by a Gibbs construction as we shall discuss below). At density ρ_{deconf} we assume a first order phase transition from confined hadronic to deconfined quark matter. Even without a matching to a hadronic model the NJL model already exhibits a transition, namely from a low density system with broken chiral symmetry to a high density system where chiral symmetry is restored. The respective density is denoted by ρ_{chiral} . For densities larger than ρ_{chiral} the Goldstone bosons which characterize the chirally broken phase are no longer stable but can decay into quark-antiquark pairs. If ρ_{chiral} was larger than ρ_{deconf} the following scenario would be conceivable: There would be three phases, namely (i) a hadronic, i.e., confined phase at low densities, (ii) a phase where quarks are deconfined but massive (in this phase, e.g., pions would still appear as bound states), and (iii) a high density phase where quarks are deconfined and their masses are so low that all mesons can decay into quarks. Had we neglected all current quark masses, the quarks in the third phase would be exactly massless. With finite current quark masses, however, the constituent quark masses keep on dropping with rising density in the third phase (cf. Fig. 3). This definitely interesting scenario with three phases is not realized in our model. It turns out that the deconfinement phase transition happens far beyond the chiral transition, i.e., $\rho_{\text{chiral}} < \rho_{\text{deconf}}$. Therefore, only the phases (i) and (iii) appear here.

In principle, since we assume the deconfinement phase transition to be of first order these two phases can coexist in a mixed phase. Indeed, it was first pointed out by Glendenning that beside a HP and a QP also this mixed phase (MP) of quark and hadronic matter may exist inside neutron stars [2,29]. (For a discussion of the geometrical structure of the MP and its consequences for the properties of neutron stars see [2].) This possibility was not realized in previous calculations due to an inadequate treatment of neutron star matter

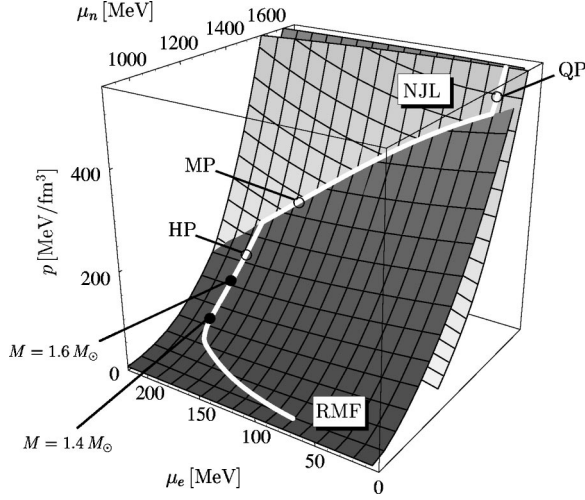


FIG. 8. Gibbs phase construction of a two-component system. Plotted is the pressure surface of the hadronic phase (RMF) and of the quark phase (NJL) as a function of the two independent chemical potentials μ_n, μ_e . EOS of the HP is GPS, EOS of the QP uses the NJL model. The white lines HP and QP show the pressure of the hadronic and the quark phase under the condition of charge neutrality. At low pressure matter is in its charge neutral HP. The intersection curve MP corresponds to the mixed phase. This curve is the solution of the Gibbs condition (21). At very high pressure matter consists of a pure QP. Also shown are the central pressures of a typical $M = 1.4M_\odot$ neutron star and of an $M = 1.6M_\odot$ star. (M_\odot denotes the mass of the sun.) Clearly neither achieves a central pressure necessary to undergo a phase transition to deconfined matter.

as a one-component system (one which can be parametrized by only one chemical potential). As we have already discussed, the treatment of neutron star matter as a charge neutral phase in weak equilibrium indeed reduces the number of independent chemical potentials to one. But the essential point is that—if a MP exists—charge neutrality can be achieved in this phase, e.g., with a positively charged amount of hadronic matter and a negatively charged amount of quark matter. Therefore it is not justified to require charge neutrality in both phases separately. In doing so we would “freeze out” a degree of freedom which in principle could be exploited in the MP by rearranging electric charge between both phases to reach “global” charge neutrality. A correct treatment of the phase transition therefore only requires both phases to be in weak equilibrium, i.e., both phases still depend on two independent chemical potentials. We have chosen the pair (μ_n, μ_e) . Such a system is called a two-component system. The Gibbs condition for mechanical and chemical equilibrium at zero temperature between both phases of the two-component system reads

$$p_{\text{HP}}(\mu_n, \mu_e) = p_{\text{QP}}(\mu_n, \mu_e) = p_{\text{MP}}. \quad (21)$$

Using Eq. (21) we can calculate the equilibrium chemical potentials of the MP where $p_{\text{HP}} = p_{\text{QP}}$ holds. Figure 8 illustrates this calculation. The HP \rightarrow MP phase transition takes place if the pressure of the charge neutral HP (white line)

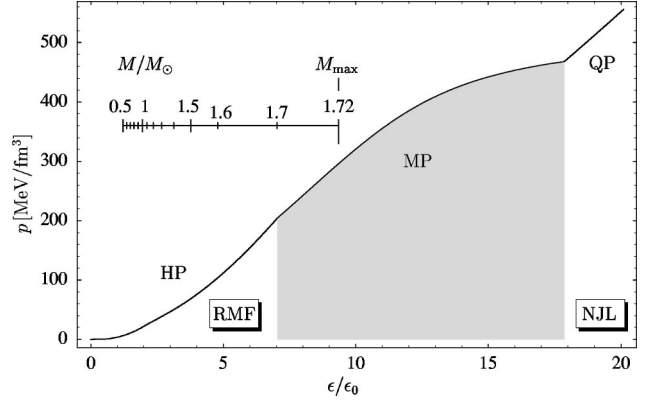


FIG. 9. EOS in the form pressure versus energy density using GPS for the hadronic EOS. The shaded region (MP) corresponds to the mixed phase part of the EOS. $\epsilon_0 = 140 \text{ MeV/fm}^3$. The mass scale in the plot shows the respective neutron star mass if the corresponding energy density is regarded as the central density of the neutron star. Obviously around the typical neutron star mass of $1.4M_\odot$ the neutron stars consist solely of hadronic matter. M_\odot denotes the mass of the sun.

meets the pressure surface of the QP (NJL). Up to this point the pressure of the QP is below the pressure of the HP making the HP the physically realized one. At higher pressure the physically realized phase follows the MP curve which is given by the Gibbs condition (21). Finally the MP curve meets the charge neutral QP curve (white line) and the pressure of the QP is above the pressure of the HP, making the QP the physically realized one. For every point on the MP curve one now can calculate the volume proportion

$$\chi = \frac{V_{\text{QP}}}{V_{\text{QP}} + V_{\text{HP}}} \quad (22)$$

occupied by quark matter in the MP by imposing the condition of global charge neutrality of the MP

$$\chi \rho_c^{\text{QP}} + (1 - \chi) \rho_c^{\text{HP}} = 0. \quad (23)$$

Here ρ_c^{QP} and ρ_c^{HP} denote the respective charge densities. From this, the energy density ϵ of the MP can be calculated by

$$\epsilon_{\text{MP}} = \chi \epsilon_{\text{QP}} + (1 - \chi) \epsilon_{\text{HP}}. \quad (24)$$

Along the MP curve the volume proportion occupied by quark matter is monotonically increasing from $\chi = 0$ to $\chi = 1$ where the transition to the pure QP takes place.

Taking (i) the charge neutral EOS of the HP at low densities (Sec. II), (ii) Eqs. (21), (23), and (24) for the MP, and (iii) the charge neutral EOS of the QP (Sec. III) we can construct the full EOS in the form $p = p(\epsilon)$. For simplicity we denote this EOS as the *hybrid star* EOS. Figure 9 shows this EOS if we apply GPS for the HP EOS. The hybrid star EOS consists of three distinct parts. At low densities ($\epsilon \lesssim 7\epsilon_0$) matter is still in its confined HP. At ($\epsilon \approx 7\epsilon_0$) the first droplets of deconfined quark matter appear. Above this den-

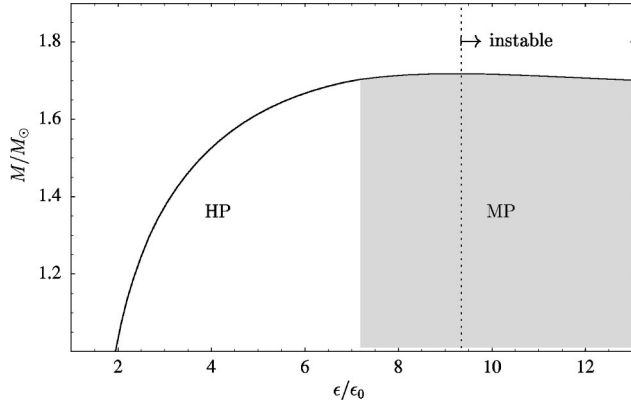


FIG. 10. Mass of the neutron star as a function of the central energy density. Above a central energy density of $\epsilon_{\text{crit}} \approx 9\epsilon_0$ where the maximum mass of the neutron star is reached the system becomes unstable with respect to radial modes of oscillations. The shaded region (MP) corresponds to stars which possess a mixed phase in their center. The hadronic part of the EOS uses GPS. $\epsilon_0 = 140 \text{ MeV/fm}^3$. M_\odot denotes the mass of the sun.

sity matter is composed of a mixed phase of hadronic and quark matter. This MP part of the EOS is shaded gray. Only at unaccessible high densities ($\epsilon \gtrsim 18\epsilon_0$) matter consists of a pure QP. The preceding statements refer to the use of GPS for the EOS of the HP. Concerning all the other variants of RMF used here (TM1, TM2, GL85) we have found that the HP \rightarrow MP transition does not appear below $\epsilon \approx 10\epsilon_0$. As we will discuss below such high energy densities cannot be reached inside a stable neutron star which is described by one of these EOS.

At this point we should note the essential difference between the treatment of neutron star matter as a one- and a two-component system (cf. [29]). While the former one leads to the well known phase transition with a constant pressure MP (like in the familiar liquid-gas phase transition of water), we can see in Fig. 9 that the pressure is monotonically increasing even in the MP if we apply the correct two-component treatment. This has an important consequence on the structure of the neutron star. Since we know from the equations of hydrostatic equilibrium—the Tolman-Oppenheimer-Volkoff (TOV) equations [28]—that the pressure has to increase if we go deeper into the star, a constant pressure MP is strictly excluded from the star while a MP with increasing pressure can (in principle) occupy a finite range inside the star.

To see if the densities inside a neutron star are high enough to establish a MP or a QP in its center we have to solve the TOV equations with a specified hybrid star EOS following from our phase transition calculation. From the solutions of the TOV equations we get a relation between the central energy density (or central pressure) and the mass of the neutron star (cf. Fig. 10). The maximum possible central energy density (the critical energy density ϵ_{crit}) is reached at the maximum mass that is supported by the Fermi pressure of the particular hybrid star EOS. Above this critical density the neutron star gets unstable with respect to radial modes of oscillations [2]. We have applied the four HP EOS's (de-

noted by GPS, TM1, TM2 and GL85) to calculate the four corresponding hybrid star EOS's. (The one for GPS is shown in Fig. 9.) We found that in *no* EOS the central energy density of a typical $M \approx 1.4M_\odot$ neutron star is large enough for a deconfinement phase transition. (Here M_\odot denotes the mass of the sun.) The corresponding neutron stars are purely made of hadronic matter (HP). In Fig. 9 where GPS is used also the neutron star masses are shown as a function of the central energy density. There the central energy density of a $M = 1.4M_\odot$ is about $\epsilon \approx 3\epsilon_0$ which is clearly below $\epsilon \approx 7\epsilon_0$ which is at least necessary to yield a MP core. (This is also shown in the context of the Gibbs construction in Fig. 8 where the central pressure of a $M = 1.4M_\odot$ and of a $M = 1.6M_\odot$ neutron star is marked.) In Fig. 9 we can see that only near the maximum mass of $M \approx 1.72M_\odot$ neutron stars with a MP core are possible. This, however, only holds for the GPS hybrid star EOS and only in a quite narrow mass range from $M \approx 1.7 - 1.72M_\odot$. In the density range up to the critical density all other EOS's (TM1, TM2, GL85) do not show a phase transition at all. The critical energy densities for these EOS's are in the range of $\epsilon_{\text{crit}} \approx 5 - 6\epsilon_0$ while the densities for the HP \rightarrow MP transition are above $\epsilon \approx 10\epsilon_0$. (The corresponding maximum masses are $M \approx 1.5 - 1.8M_\odot$.) Up to now we have concentrated on the bulk properties of the phases which constitute the mixed phase while neglecting Coulomb and surface effects. The additional inclusion of such effects [30] would cause the MP to become even more disfavored. From this we conclude that within the model constructed here the appearance of deconfined quark matter in the center of neutron stars turns out to be very unlikely.

V. SUMMARY AND CONCLUSIONS

We have studied the possible phase transition inside neutron stars from confined to deconfined matter. For the description of the quark phase we have utilized the NJL model which respects chiral symmetry and yields dynamically generated quark masses via the effect of spontaneous chiral symmetry breaking. Concerning the application to neutron stars this provides a completely novel approach beyond the usually utilized Bag model type equations of state. We found that the appearance of deconfined quark matter in the center of a neutron star appears to be very unlikely, for most of the studied hadronic EOS's even impossible. The ultimate reason for that effect is the high value of the effective strange quark mass which turns out to be much higher than its current mass value in the whole relevant density range (cf. Fig. 3). This finding, of course, is based on several assumptions which need not necessarily be correct. In lack of an EOS based on a full QCD calculation at zero temperature and finite nuclear density, we had to rely on simpler models for the EOS in different density regimes.

Concerning the low density regime we have used various relativistic mean field (RMF) models. To some degree the use of different variants of the RMF model should reflect the uncertainties of this approach. These models are generalizations of the Walecka model [31] which describes the hadronic ground state of nuclear matter at density ρ_0 quite suc-

cessfully. At somewhat higher densities the used RMF models deal with hyperons as additional degrees of freedom. Since these RMF models do not have any explicit quark degrees of freedom we expect them to become unreliable at high densities where the confinement forces are screened and the hadrons dissolve into quarks.

To describe this high density regime we have utilized the Nambu–Jona-Lasinio (NJL) model in its three-flavor extension. The merits of the NJL model are (at least) twofold: For the vacuum case, it gives a reasonable description of spontaneous chiral symmetry breaking and of the spectrum of the low lying mesons. For sufficiently high density and/or temperature, the NJL model exhibits the restoration of chiral symmetry. A shortcoming of the NJL model is that it does not confine quarks, i.e., there is no mechanism which prevents the propagation of a single quark in vacuum. Therefore in an NJL model calculation the quarks significantly contribute to the EOS also at low densities.¹ This was the ultimate reason why we considered the NJL model only in the high density regime where confinement is supposed to be absent anyway while utilizing the hadronic RMF models to describe the confined phase. On the other hand, we should recall that energy density and pressure of the NJL model were determined such that both vanish at zero density, i.e., in a regime where we have not utilized the NJL model afterwards. This procedure determines the effective bag pressure B_{eff} given in Eq. (9) by fixing B_0 (11) to $(217.6 \text{ MeV})^4$. Clearly, this procedure is somewhat unsatisfying since the effective bag pressure B_{eff} influences the EOS and therefore the onset of the phase transition. Indeed, if we reduce B_0 by only 5–10% by hand from its original value of $(217.6 \text{ MeV})^4$ we already observe drastic changes in the phase structure of the neutron star favoring deconfined quark matter. On the other hand, the physical requirement that any model should yield vanishing energy density and pressure in vacuum is the only way to uniquely determine the EOS of the NJL model without any further assumptions. We have also investigated the sensitivity of our results to an increase of the cutoff parameter Λ . As mentioned in Sec. III this cutoff $\Lambda = 602.3 \text{ MeV}$ is comparatively low. However, we found that an artificial increase of Λ leads to an increase of the effective bag constant and the effective quark masses. According to the considerations presented above it is obvious that in this case the appearance of quark matter inside of neutron stars becomes even less likely. On the other hand, we note that the choice for the cutoff (and for the other parameters of the NJL model) is by no means arbitrary but chosen such that the vacuum properties of the pseudoscalar mesons are correctly reproduced (cf. Sec. III). Thus, a change of the cutoff should come along with an appropriate change of the other parameters to reproduce the physical meson properties. For example, we have also explored the set given in [37] with a somewhat larger cutoff: $\Lambda = 631 \text{ MeV}$, $G\Lambda^2 = 1.830$, $K\Lambda^5 = 9.19$, $m_q = 5.5$

MeV, and $m_s = 138 \text{ MeV}$. The results are very similar to the ones presented here.

Possible alternatives to the use of the NJL model for the description of the deconfined quark matter are the MIT bag model [2] and the extended effective mass bag model [26,27]. The latter includes medium effects due to one-gluon exchange which rise with density (while the effective masses of the NJL model decrease). As already discussed at the end of Sec. III for the regime of very high densities such a resummed perturbation theory might be more adequate. Furthermore, MIT bag models can be very useful in interpreting more involved models like the NJL model in terms of simple physical quantities like the bag constant and the quark masses. Therefore we have frequently compared our NJL model results with the MIT bag model in Sec. III. For a further discussion of the MIT bag model and its application to neutron stars see [32].

The distinct feature of the NJL model is that nonperturbative effects are still present beyond the phase transition point. It is reasonable to consider such effects since it was found in lattice calculations [33,34] that for QCD at finite temperature the EOS beyond the phase transition point can neither be properly described by a free gas of quarks and gluons nor by QCD perturbation theory [35,36]. Presumably this holds also for the finite density regime. On the mean field level the most prominent nonperturbative feature of the NJL model which remains present beyond the phase transition point is the constituent strange quark mass which is much larger than the current strange quark mass in the whole relevant density regime (cf. Fig. 3). This high strange quark mass has turned out to be crucial for the phase transition. As we have shown above the EOS of the QP can be reasonably well approximated by an MIT bag EOS up to 5 times ρ_0 using a comparatively low bag constant of $B_{\text{MIT}}^{1/4} = 170 \text{ MeV}$ and an effective strange quark mass of $m_s^{\text{MIT}} = 465 \text{ MeV}$. These are the plateau values of the corresponding quantities in the NJL model calculations shown in Figs. 3 and 4. In Figs. 5–7 the curves labeled by MIT use these values for the bag constant and the effective strange quark mass. Using such a bag constant in connection with the *current* strange quark mass would allow the existence of a QP inside a neutron star [2,32]. This, however, does not remain true once a much higher effective strange quark mass is used. Qualitatively, the chain of arguments is that a higher mass leads to a lower pressure (cf. Fig. 6). This disfavors the quark phase in the Gibbs construction, i.e., shifts the phase transition point to higher densities. This is the reason why in our calculations the existence of quark matter in the center of a neutron star is (nearly) excluded. Especially for typical neutron stars with masses $M \approx 1.4M_\odot$ the central energy density is far below the deconfinement phase transition density (cf. Fig. 7). This finding is independent of the choice of the version of the RMF model. This suggests that it is the NJL model with its large strange quark mass which defers the onset of the deconfinement phase transition rather than the modeling of the hadronic phase.

For simplicity we have treated in the present work the NJL model in the Hartree approximation. In principle, going beyond the mean field approximation might influence the

¹Actually in the mean field approximation the quarks are the only degrees of freedom which contribute. For a generalization to include meson states as RPA modes in the NJL EOS see [24,25].

order of the chiral phase transition (for related work towards that direction for the two-flavor case cf. [38]). If it turned out that this would result in a strong first order phase transition then the effective strange quark mass might change more drastically and in the region of interest would be perhaps much lower than in the case studied in the present work. This would favor the appearance of quark matter in the interior of neutron stars. Clearly, it would be interesting to study how a more involved treatment of the NJL model beyond the Har-

tree approximation would influence our findings presented here. This, however, is beyond the scope of the present work.

ACKNOWLEDGMENTS

The authors thank C. Greiner and M.H. Thoma for helpful discussions and for reading the manuscript. We also acknowledge discussions with M. Hanauske. The work of K.S. is supported by DFG.

-
- [1] S.L. Shapiro and S.A. Teukolsky, *Black Holes, White Dwarfs, and Neutron Stars* (Wiley, New York, 1983).
- [2] N.K. Glendenning, *Compact Stars* (Springer-Verlag, New York, 1997).
- [3] A. Chodos, R.L. Jaffe, K. Johnson, C.B. Thorn, and V.F. Weisskopf, Phys. Rev. D **9**, 3471 (1974); A. Chodos, R.L. Jaffe, K. Johnson, and C.B. Thorn, *ibid.* **10**, 2599 (1974).
- [4] E. Farhi and R.L. Jaffe, Phys. Rev. D **30**, 2379 (1984).
- [5] A.R. Bodmer, Phys. Rev. D **4**, 1601 (1971).
- [6] E. Witten, Phys. Rev. D **30**, 272 (1984).
- [7] *Strange Quark Matter in Physics and Astrophysics*, Aarhus, Denmark, 1991, edited by J. Madsen and P. Haensel [Nucl. Phys. B (Proc. Suppl.) **24B** (1991)].
- [8] M. Buballa and M. Oertel, hep-ph/9810529.
- [9] U. Vogl and W. Weise, Prog. Part. Nucl. Phys. **27**, 195 (1991).
- [10] S.P. Klevansky, Rev. Mod. Phys. **64**, 649 (1992).
- [11] T. Hatsuda and T. Kunihiro, Phys. Rep. **247**, 221 (1994).
- [12] R.J. Furnstahl, H.-B. Tang, and S.D. Serot, Phys. Rev. C **52**, 1368 (1995); R.J. Furnstahl, S.D. Serot, and H.-B. Tang, Nucl. Phys. **A615**, 441 (1997); **A640**, 505(E) (1998).
- [13] P. Papazoglou, S. Schramm, J. Schaffner-Bielich, H. Stöcker, and W. Greiner, Phys. Rev. C **57**, 2576 (1998); P. Papazoglou, D. Zschesche, S. Schramm, J. Schaffner-Bielich, H. Stöcker, and W. Greiner, *ibid.* **59**, 411 (1999).
- [14] H. Müller, Phys. Rev. C **59**, 1405 (1999).
- [15] M. Hanauske (private communication).
- [16] G. Baym, C.J. Pethick, and P. Sutherland, Astrophys. J. **170**, 299 (1971); R.P. Feynman, N. Metropolis, and E. Teller, Phys. Rev. **75**, 1561 (1949); G. Baym, H.A. Bethe, and C.J. Pethick, Nucl. Phys. **A175**, 225 (1971).
- [17] H. Shen, H. Toki, K. Oyamatsu, and K. Sumiyoshi, Nucl. Phys. **A637**, 435 (1998).
- [18] N.K. Glendenning, F. Weber, and S.A. Moszkowski, Nucl. Phys. **A572**, 693 (1994); J.I. Kapusta and K.A. Olive, Phys. Rev. Lett. **64**, 13 (1990); J. Ellis, J.I. Kapusta, and K.A. Olive, Nucl. Phys. **B348**, 345 (1991).
- [19] N.K. Glendenning, Phys. Lett. **114B**, 392 (1982); Z. Phys. A **327**, 295 (1987).
- [20] J. Schaffner and I.N. Mishustin, Phys. Rev. C **53**, 1416 (1996).
- [21] S.K. Ghosh, S.C. Phatak, and P.K. Sahu, Z. Phys. A **352**, 457 (1995).
- [22] Y. Nambu and G. Jona-Lasinio, Phys. Rev. **122**, 345 (1961); **124**, 246 (1961).
- [23] P. Rehberg, S.P. Klevansky, and J. Hüfner, Phys. Rev. C **53**, 410 (1996).
- [24] J. Hüfner, S.P. Klevansky, P. Zhuang, and H. Voss, Ann. Phys. (N.Y.) **234**, 225 (1994).
- [25] P. Zhuang, J. Hüfner, and S.P. Klevansky, Nucl. Phys. **A576**, 525 (1994).
- [26] K. Schertler, C. Greiner, and M.H. Thoma, Nucl. Phys. **A616**, 659 (1997).
- [27] K. Schertler, C. Greiner, P.K. Sahu, and M.H. Thoma, Nucl. Phys. **A637**, 451 (1998).
- [28] J.R. Oppenheimer and G.M. Volkoff, Phys. Rev. **55**, 347 (1939).
- [29] N.K. Glendenning, Phys. Rev. D **46**, 1274 (1992).
- [30] H. Heiselberg, C.J. Pethick, and E.F. Staubo, Phys. Rev. Lett. **70**, 1355 (1993).
- [31] B.D. Serot and J.D. Walecka, Adv. Nucl. Phys. **16**, 1 (1986).
- [32] K. Schertler, J. Schaffner-Bielich, C. Greiner, and M.H. Thoma (in preparation).
- [33] C. DeTar, in *Quark-Gluon Plasma 2*, edited by R.C. Hwa (World Scientific, Singapore, 1995), p. 1.
- [34] E. Laermann, Nucl. Phys. **A610**, 1c (1996).
- [35] C. Zhai and B. Kastening, Phys. Rev. D **52**, 7232 (1995).
- [36] E. Braaten and A. Nieto, Phys. Rev. D **53**, 3421 (1996).
- [37] T. Kunihiro, Phys. Lett. B **219**, 363 (1989).
- [38] J. Berges, D.-U. Jungnickel, and C. Wetterich, hep-ph/9811347.